Hindawi Publishing Corporation
International Journal of Antennas and Propagation
Volume 2011, Article ID 756153, 11 pages
doi:10.1155/2011/756153

Research Article

Wideband Analysis of Mutual Coupling Compensation Methods

Simon Henault and Yahia M. M. Antar

Department of Electrical and Computer Engineering, Royal Military College of Canada, Kingston, ON, Canada K7K 7B4

Correspondence should be addressed to Simon Henault, henault@rmc.ca

Received 30 April 2011; Accepted 21 June 2011

Academic Editor: Hon Tat Hui

The performance of various mutual coupling estimation and compensation methods is quantified and compared for wideband operation. Their main limitations and the required procedures to estimate the coupling matrix are outlined. It is determined that only the full-wave method is accurate at all frequencies. The performance tradeoffs associated with the other methods are described. General guidelines based on the electrical size and separation of the array elements are formulated for each method. The results can be valuable for both wideband and narrowband receiving antenna arrays.

1. Introduction

Mutual coupling in antenna arrays is a subject that has received considerable attention in recent years. With the increase in signal processing capabilities, smart antennas are a promising technology that seeks the optimization of signal reception through spatial processing and other means. For example, with the knowledge of the relative phase shifts between the elements of an array, it is possible to maximize the received power, minimize interference, and estimate the direction of arrival (DOA) of impinging signals. However, due to the relatively small spacings between the elements, which is generally required to achieve some of the above goals, electromagnetic interactions between the array elements appear which lead to mutual coupling effects.

It is widely acknowledged that mutual coupling may severely impact the performance of smart antennas. To mitigate the effects of mutual coupling, several methods have been proposed in the literature. These methods generally attempt to estimate the coupling matrix describing the mutual coupling. The coupling matrix is subsequently used by the signal processor to compensate for the effects of mutual coupling. A comprehensive review of mutual coupling compensation (MCC) methods available in the scientific literature was done in [1]. These methods typically use different approaches to estimate the coupling matrix. Previously published work that originally introduced the different MCC methods [2–5] and subsequent published work (see [1]) based on these methods reported significant performance improvements by the implementation of MCC in applications of beamforming and direction of arrival estimation. Although mutual coupling is highly dependent on frequency, the studies performed to this date are limited to the narrowband case where operation for a single frequency was evaluated. Besides the summarized results of [6], no work has been published on the performance of MCC methods for wideband applications.

Through the wideband performance evaluation of the various available MCC methods, it is expected that one will be able to determine their limitations. The aim of this paper is twofold. First, to show the limitations of each of the MCC methods. Second, to accurately quantify and compare the performance of the MCC methods for both wideband and narrowband applications. The paper is organized as follows. In Section 2, the theoretical development of the MCC methods is reviewed. The performance of the different methods is calculated numerically in Section 3 for a known elevation angle, while it is evaluated in Section 4 for an unknown elevation angle. Finally, conclusions are presented in Section 5.

2. Mutual Coupling Compensation Methods

The four main MCC methods, as described in [1], are reviewed in this section. They are treated in the chronological

order in which they appeared in the scientific literature. In each of the four methods, the coupled signals are related to the uncoupled signals by the following equation:

$$\mathbf{v} = C\mathbf{v_{ideal}}, \tag{1}$$

where $\mathbf{v}$ is a column vector containing the coupled signals, $\mathbf{v_{ideal}}$ is a column vector containing the uncoupled signals, and C is the coupling matrix. With the knowledge of C, the uncoupled signals can be retrieved using

$$\mathbf{v_{ideal}} = C^{-1}\mathbf{v}. \tag{2}$$

The coupled signals of $\mathbf{v}$ are the terminal voltages measured across the load impedances connected to the terminals of the elements, and the uncoupled signals of $\mathbf{v_{ideal}}$ are the incident signals at each of the elements. Therefore, (2) implies that the incident signals are retrieved by simply multiplying the inverse of the coupling matrix by the terminal voltage vector. In practical situations, the coupling matrix is not necessarily perfectly known, and the incident signals are estimated as follows:

$$\widetilde{\mathbf{v}}_{\mathbf{ideal}} = \widetilde{C}^{-1}\mathbf{v}, \tag{3}$$

where $\widetilde{C}$ is the estimated coupling matrix, and $\widetilde{\mathbf{v}}_{\mathbf{ideal}}$ is the estimated incident signal vector. The accuracy of $\widetilde{\mathbf{v}}_{\mathbf{ideal}}$ is thus dependent upon the MCC method used in the calculation of $\widetilde{C}$.

2.1. Open-Circuit Voltage Method. The open-circuit voltage method was originally suggested in [2] in 1983. The method is based on the assumption that the open-circuit equivalent voltage of each array element is independent of mutual coupling. Therefore, (1) is assumed to be equivalent to

$$\mathbf{v} = \widetilde{C}\mathbf{v_{oc}}, \tag{4}$$

where $\mathbf{v_{oc}}$ is the open-circuit equivalent voltage vector. These voltages are believed to be the voltages that would be measured at the terminals of the elements if the load impedances were removed. The estimated coupling matrix is given by

$$\widetilde{C} = Z_L(Z_L + Z)^{-1}, \tag{5}$$

where Z_L is a diagonal matrix whose entries are the individual load impedances connected to the elements, and Z is the mutual impedance matrix. The induced electromotive force (emf) method, introduced in [7] in 1932, can be used to calculate the entries of Z. For vertical centrally terminated thin dipoles, centered at $z = 0$, the entries of Z can, therefore, be calculated using the following equation:

$$Z_{ij} = -\frac{1}{I_i(0)I_j(0)}\int_{-L_i/2}^{L_i/2} E_{j_z}(z)I_i(z)dz, \tag{6}$$

where $I_i(z)$ is the current distribution along element i when it is excited by a voltage source at its terminals, E_{j_z} is the electric field at the surface of element i resulting from the excitation of element j by a voltage source at its terminals, L_i is the physical length of element i, and $I_i(0)$ and $I_j(0)$ are the respective input currents of elements i and j when separately excited by a voltage source while the terminals of the other are short circuited.

When L_i is approximately equal to half a wavelength ($L_i \approx \lambda/2$), it is often assumed that the amplitude of $I_i(z)$ is sinusoidally distributed, and the phase is constant over z. Based on this assumption, analytical expressions can be obtained for the mutual impedances [8]. However, the assumption is violated for elements that are not infinitely thin, such as practical elements. Moreover, the assumption is narrowband in nature and is not valid for a wideband analysis of mutual coupling. Therefore, alternate calculation techniques are required to solve for the current distributions. Numerical techniques such as the method of moments (MoM) [9] can be used to calculate the theoretical mutual impedances of the array. To avoid having to first solve for the current distributions, calculate the electric fields, and then use (6) to finally obtain the mutual impedances; there are some alternatives. One of these is to separately excite the elements by a voltage source (V_j) and find the induced current at the shorted terminals (I_i) of the other elements calculated using the numerical technique. Then, the mutual admittances are simply calculated using

$$Y_{ij} = \frac{I_i}{V_j}. \tag{7}$$

The mutual impedance matrix is then calculated with

$$Z = Y^{-1}. \tag{8}$$

It is noted that the procedure described here lends itself well to experimental implementation where numerical calculations can be avoided completely. Alternatively, a vector network analyzer (VNA) can be used to measure the scattering parameters between the elements, and the mutual impedance matrix can be calculated with

$$Z = Z_o(I + S)(I - S)^{-1}, \tag{9}$$

where S is the scattering matrix containing the scattering parameters, Z_o is the reference impedance used in the measurement of S, and I is the identity matrix.

The deficiencies of the open-circuit voltage method were outlined in [4, 5] and in numerous publications reviewed in [1]. The main problem with the method is that it assumes that the excitation of the array occurs only at the terminals of the elements. While this is usually true for a transmitting array, it is not for a receiving array. The excitation of a receiving array is generally the external illumination of the elements by incident uniform plane waves, which occurs along the entire surfaces of the elements and not only at their terminals. The open-circuit voltage method, therefore, appears to be more suitable for characterizing mutual coupling in transmitting antenna arrays since they are excited by discrete sources at the terminals of the elements [10]. Since the external illumination of a receiving array consisting of electrically small elements can be approximated as the discrete

excitation of the terminals of each element, the method is also appropriate for this type of array used in the receiving mode. A proof of this is presented in Section 2.3.

2.2. Calibration Method. The calibration method was first used in [3] in 1991. It consists in the sequential calculation or measurement of the terminal voltage vector $\mathbf{v}$, in response to the external plane wave illumination of the array from a discrete number of calibration points corresponding to different DOAs. For each of the individual calibration points, the terminal voltage vector is governed by (1). The terminal voltage vectors for all the calibration points are combined to form matrix V as follows:

$$V = \left[\mathbf{v_1} \;\; \mathbf{v_2} \;\; \cdots \;\; \mathbf{v_M}\right], \tag{10}$$

where $\mathbf{M}$ is the number of calibration points. Based on the knowledge of the individual DOAs of the calibration points, the matrix V_{ideal} is formed as follows:

$$V_{\text{ideal}} = \left[\mathbf{v_{ideal_1}} \;\; \mathbf{v_{ideal_2}} \;\; \cdots \;\; \mathbf{v_{ideal_M}}\right]. \tag{11}$$

For an infinite number of different calibration points, (10) is related to (11) by the following equation:

$$V = CV_{\text{ideal}}. \tag{12}$$

However, in practical situations, the number of different calibration points is finite, and (12) becomes

$$V = \widetilde{C}V_{\text{ideal}}. \tag{13}$$

Therefore, the coupling matrix is estimated by the least-square solution of (13) given by

$$\widetilde{C} = V{V_{\text{ideal}}}^H\left(V_{\text{ideal}}{V_{\text{ideal}}}^H\right)^{-1}, \tag{14}$$

where ${V_{\text{ideal}}}^H$ denotes the Hermitian transpose of V_{ideal}. A necessary condition for obtaining a unique solution is that the number of different calibration points must be at least equal to the number of array elements [3].

In comparison to the open-circuit voltage method, the calibration method is more suitable for the characterization of mutual coupling in receiving arrays since $\widetilde{C}$ is calculated using vectors obtained in the receiving mode. The accuracy of $\widetilde{C}$ depends on both the complexity of the antenna array and the number of calibration points. An interesting aspect of the calibration method is that it can completely be implemented experimentally and yield an accurate estimate of the coupling matrix if the number of calibration points is sufficient. However, the procedures involved in the determination of the terminal voltage vectors, either through experimental measurements or numerical calculations, can be tedious.

2.3. Full-Wave Method. The full-wave method was formulated in [4] in 2000. The method directly uses the interaction matrix numerically calculated by the method of moments (MoM). The MoM requires the array elements to be discretized into electrically small segments in order to solve for the current distribution resulting from an excitation. As an example, Figure 1 shows a single dipole, discretized into K segments of length Δz, centrally terminated into the load impedance Z_L. The MoM yields a convenient matrix equation that relates the excitations to the currents

$$\mathbf{v_{MoM}} = Z_{\text{MoM}}\mathbf{i}, \tag{15}$$

where $\mathbf{v_{MoM}}$ is the excitation vector whose entries are the excitation of each of the segments, $\mathbf{i}$ is the current vector whose entries are the currents on each segment, and Z_{MoM} is the interaction matrix. To calculate currents based on a known excitation, (15) is inverted to give

$$\mathbf{i} = Y_{\text{MoM}}\mathbf{v_{MoM}}, \tag{16}$$

where $Y_{\text{MoM}} = {Z_{\text{MoM}}}^{-1}$.

For clarity, the full-wave method was illustrated in [4] using an array of two elements comprised of three segments each. Here, the method is generalized to an arbitrary number of vertical wire elements having an arbitrary number of segments. The excitation vector is proportional to the incident signals illuminating the segments and can, therefore, be expressed as

$$\mathbf{v_{MoM}} = \left[\mathbf{v_1} \;\; \mathbf{v_2} \;\; \cdots \;\; \mathbf{v_N}\right]^T, \tag{17}$$

where $[\cdot]^T$ denotes the transpose operation, N is the number of array elements, and

$$\mathbf{v_i} = V_i\mathbf{\Phi_i}, \tag{18}$$

where

$$\mathbf{\Phi_i} = \left[e^{j(2\pi/\lambda)z_i^1\cos\theta}e^{j(2\pi/\lambda)z_i^2\cos\theta}\cdots e^{j(2\pi/\lambda)z_i^{K_i}\cos\theta}\right]. \tag{19}$$

This formulation is valid for the illumination of the array by plane waves since the excitation of the segments of a given element, i, only varies as a function of θ, λ, and the vertical position of the segments given by z_i^k. The superscript k used in the latter expression designates the segment number for element i, and its largest value is given by K_i. The common term V_i is a complex scalar value proportional to the external excitation of element i based on its horizontal position. Here, it is important to note the following relation with respect to the incident signal vector discussed in Section 2

$$\mathbf{v_{ideal}} = \left[V_1 \;\; V_2 \;\; \cdots \;\; V_N\right]^T. \tag{20}$$

The entries of Y_{MoM} relating the incident signals to the terminal currents are given by the rows of Y_{MoM} whose indexes correspond to the segment indexes of the terminals. These rows are used to form Y_T in the new equation for the terminal currents

$$\mathbf{i_T} = Y_T\mathbf{v_{MoM}}. \tag{21}$$

By subdividing matrix Y_T into N^2 row vectors $\mathbf{y_{ij}}$ comprised of K_j entries and substituting (17) into (21), (21) can be expressed as

$$\mathbf{i_T} = Y'_T\mathbf{v_{ideal}}, \tag{22}$$

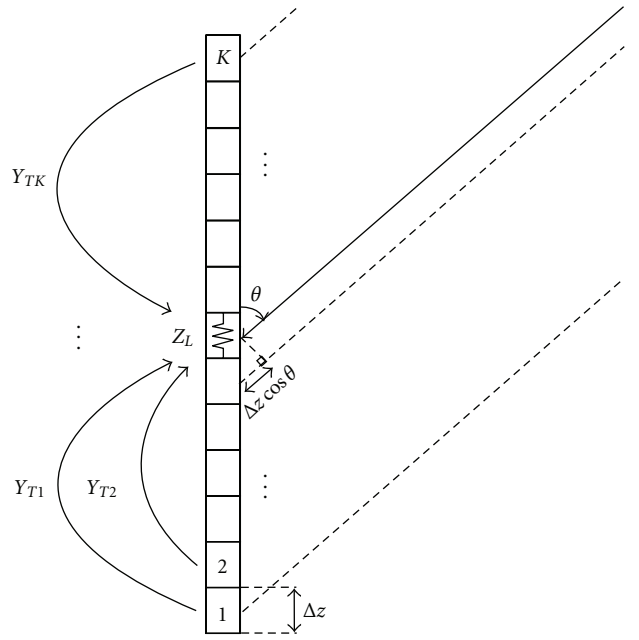

Figure 1: Geometry of the full-wave method for a single vertical dipole, centrally terminated into load impedance Z_L, discretized into K segments having an equal length of Δz, and illuminated by a plane wave arriving from an elevation angle θ. The coefficients Y_{Tk} describe the interactions between the excitation of segment k by the plane wave and the dipole terminals.

where

$$Y_T' = \begin{bmatrix} \mathbf{y_{11}\Phi_1}^T & \mathbf{y_{12}\Phi_2}^T & \cdots & \mathbf{y_{1N}\Phi_N}^T \\ \mathbf{y_{21}\Phi_1}^T & \mathbf{y_{22}\Phi_2}^T & \cdots & \mathbf{y_{2N}\Phi_N}^T \\ \vdots & \vdots & \ddots & \vdots \\ \mathbf{y_{N1}\Phi_1}^T & \mathbf{y_{N2}\Phi_2}^T & \cdots & \mathbf{y_{NN}\Phi_N}^T \end{bmatrix}. \quad (23)$$

The terminal voltages are given by

$$\mathbf{v} = Z_L \mathbf{i_T}, \quad (24)$$

where Z_L is a diagonal matrix whose entries are the individual load impedances at the terminals of each element. Substituting (22) into (24) gives

$$\mathbf{v} = Z_L Y_T' \mathbf{v_{ideal}}. \quad (25)$$

It follows that the coupling matrix is estimated using

$$\widetilde{C} = Z_L Y_T'. \quad (26)$$

The main advantage of the full-wave method is that the coupling matrix estimate is very accurate provided that the MoM numerical model is also accurate. However, the *a priori* knowledge of the elevation angle of incoming signals is required to compute $\widetilde{C}$. An equivalent method not limited to the MoM has been presented in [11].

An interesting case occurs for electrically small elements, where a single segment per element is required for the accurate calculation of $\widetilde{C}$. When this condition is satisfied, Z_{MoM} is given by [8]

$$Z_{\text{MoM}} = \begin{bmatrix} Z_{11} + Z_{L_1} & Z_{12} & \cdots & Z_{1N} \\ Z_{21} & Z_{22} + Z_{L_2} & \cdots & Z_{2N} \\ \vdots & \vdots & \ddots & \vdots \\ Z_{N1} & Z_{N2} & \cdots & Z_{NN} + Z_{L_N} \end{bmatrix}. \quad (27)$$

If Z is defined as the Z_{MoM} matrix when all the elements are short circuited, that is, $Z_{L_1} = Z_{L_2} = \cdots = Z_{L_N} = 0$, then using (15), it is seen that

$$\begin{aligned} \mathbf{v} &= Z_L \mathbf{i} \\ &= Z_L {Z_{\text{MoM}}}^{-1} \mathbf{v_{MoM}} \\ &= Z_L (Z_L + Z)^{-1} \mathbf{v_{MoM}}. \end{aligned} \quad (28)$$

For a single segment per element, $\mathbf{v_{MoM}} = \mathbf{v_{ideal}}$, and (28) becomes

$$\mathbf{v} = Z_L (Z_L + Z)^{-1} \mathbf{v_{ideal}}. \quad (29)$$

This equation is similar to (4)-(5). Therefore, the open-circuit voltage method is accurate for arrays of electrically small elements.

2.4. Receiving Mutual Impedance Method. The receiving mutual impedance method was proposed in [5] in 2003. In an attempt to address the main deficiency of the open-circuit voltage method of inaccurately modeling receiving arrays, the method involves a new definition of mutual impedances. Instead of calculating the mutual impedances in the transmission mode, they are calculated in the receiving mode under external plane wave excitation. The mutual impedances are then given by

$$Z_{ij} = \frac{V_{ij}}{I_j}, \quad (30)$$

for $i \neq j$, where I_j is the current induced in Z_{L_j} by the external plane wave, and V_{ij} is the voltage induced across Z_{L_i}, that is solely due to the excitation of element j. Hence, the procedure involved for computing V_{ij} in (30) requires the subtraction of the induced voltage across Z_{L_i} in the absence of element j from the induced voltage across Z_{L_i} in the presence of element j. By superposition, the terminal voltages are given by

$$V_i = V_{\text{ideal}_i} + \sum_{i \neq j} Z_{ij} I_j. \quad (31)$$

Substituting $I_j = V_j / Z_{L_j}$ into (31), the incident signals are given by

$$V_{\text{ideal}_i} = V_i - \sum_{i \neq j} \frac{Z_{ij}}{Z_{L_j}} V_j. \quad (32)$$

Equation (32) can be expressed in the following convenient matrix equation:

$$\mathbf{v} = \widetilde{C}\mathbf{v}_{\mathbf{ideal}}, \tag{33}$$

where

$$\widetilde{C} = \begin{bmatrix} 1 & -\frac{Z_{12}}{Z_{L_2}} & \cdots & -\frac{Z_{1N}}{Z_{L_N}} \\ -\frac{Z_{21}}{Z_{L_1}} & 1 & \cdots & -\frac{Z_{2N}}{Z_{L_N}} \\ \vdots & \vdots & \ddots & \vdots \\ -\frac{Z_{N1}}{Z_{L_1}} & -\frac{Z_{N2}}{Z_{L_2}} & \cdots & 1 \end{bmatrix}^{-1}. \tag{34}$$

The receiving mutual impedance method was demonstrated to be superior to the open-circuit voltage method in applications of direction finding and adaptive nulling [1]. Similar to the open-circuit and calibration methods, it is well suited for practical implementation where the mutual impedances of (30) can be measured instead of being calculated numerically. In comparison with the full-wave method, it claims to offer the additional advantage of not requiring *a priori* knowledge of the elevation angle of incoming signals. However, this relies on the assumption that the current distributions remain unchanged irrespective of the elevation angle. As acknowledged in [12], this is not necessarily true. Moreover, the currents in (31) are assumed to be equal to those in (30) despite the presence of only two elements in the latter equation and of all the elements in the former equation. This problem was addressed in the new mutual impedance calculation approach presented in [13, 14]. This approach elegantly reduces the number of coupling parameters that must be estimated in the calibration method described in Section 2.2, reducing the minimum number of calibration points to $N - 1$. Consequently, its performance is more an improvement of the calibration method than it is an improvement of the receiving mutual impedance method, despite its name. It is also assumed in the receiving mutual impedance method that the current distributions used in (30) are independent of the DOA of the external excitation. These assumptions may be violated when the elements are very closely spaced. Therefore, the method cannot be expected to provide an accurate estimate of the coupling matrix for arbitrary frequencies and array configurations.

3. Performance Comparison of Mutual Coupling Compensation Methods

To evaluate the wideband performance of the MCC methods discussed in Section 2, simple dipoles are selected. Although dipoles are generally not used in wideband applications, they are nevertheless a useful tool for the performance analysis at multiple frequencies due to their simplicity. Also, for applications such as wideband direction finding, they are often employed to cover bandwidths exceeding 5 : 1. Their individual performance can be measured by their realized gain [15], which takes into account both the impedance mismatch and the gain in the direction of interest. It is, therefore, a measure of performance in comparison to a hypothetical perfectly matched isotropic antenna. The realized gain is given by

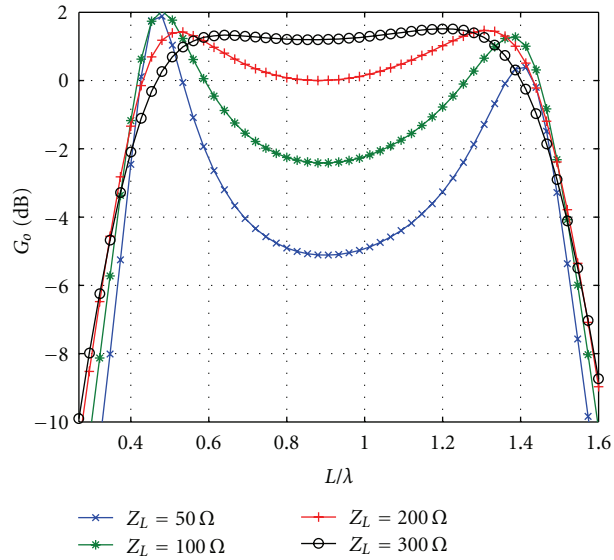

Figure 2: Realized gain of a single vertical dipole of length equal to 1.6 times the smallest operating wavelength, centrally terminated into various values of load impedance Z_L.

$$G_o(\phi,\theta) = \left(1 - |\Gamma|^2\right) G(\phi,\theta), \tag{35}$$

where $G(\phi,\theta)$ is the directional gain, and Γ is the reflection coefficient resulting from the impedance mismatch. The latter is given by

$$\Gamma = \frac{Z_L - Z_{\text{ANT}}}{Z_L + Z_{\text{ANT}}}, \tag{36}$$

where Z_{ANT} is the input impedance of the antenna and Z_L is the load impedance connected to its terminals. It is verified that a perfectly matched isotropic antenna yields unity in (35). The realized gain of a dipole antenna having a length of $1.6\lambda_o$ and a radius of $\lambda_o/200$, where λ_o is the smallest wavelength of interest, and centrally terminated into various values of load impedance Z_L, is shown in Figure 2. The minimum acceptable realized gain is dependent upon the intended application. In applications of wideband direction finding, for example, a minimum value of -10 dB is often accepted. The realized gain of Figure 2 is calculated using the MoM-based numerical electromagnetic code (NEC) [16] for $\theta = 90°$. Since only the performance of a single dipole is calculated, it is independent of azimuth angle. It is seen that using a large value of load impedance raises the realized gain between the first two resonances of the dipole at $L \approx 0.5\lambda$ and $L \approx 1.3\lambda$. Load impedances of $300\,\Omega$ are, therefore, used in the remainder of this paper. An interesting advantage of operating near the second resonance can be observed in Figure 2 since the realized gain is maximum at $L \approx 1.2\lambda$ due to the maximum directional gain achieved at this frequency.

For the wideband analysis, a planar array of nine of these dipoles is used, as illustrated in Figure 3. To avoid grating

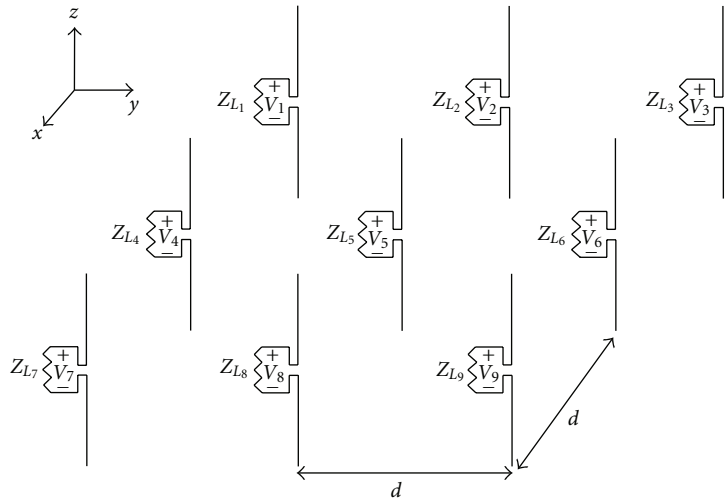

Figure 3: Nine-dipole array geometry used for the wideband analysis. The dipoles are placed in a planar array arrangement where the separation between them is given by d. The terminal voltages are measured across the load impedances located at the center of each of the dipoles.

lobes for any steering direction, the separation between the elements is fixed to $d = 0.5\lambda_o$. Smart antennas generally aim at maximizing the output signal-to-noise ratio (SNR). A common measure of their effectiveness in achieving this goal is the array gain given by [17]

$$A = \frac{\text{SNR}_{\text{out}}}{\text{SNR}_{\text{in}}}, \tag{37}$$

where SNR_{in} and SNR_{out} are the SNRs at the input and output of the signal processor, respectively. In the presence of receiver noise with no interferers, the terminal voltages are described by

$$\mathbf{v} = \mathbf{s} + \mathbf{n}, \tag{38}$$

where $\mathbf{s} = C\mathbf{v}_{\mathbf{ideal}}$, and the column vector $\mathbf{n}$ contains the noise at each array element. The SNR_{in} in (37) is obtained using the entries of $\mathbf{v}$ in (38)

$$\text{SNR}_{\text{in}} = E\left(\frac{\sum_{i=1}^{N}|s_i|^2}{\sum_{i=1}^{N}|n_i|^2}\right) = E\left(\frac{\mathbf{v}_{\mathbf{ideal}}{}^H C^H C\mathbf{v}_{\mathbf{ideal}}}{\mathbf{n}^H\mathbf{n}}\right), \tag{39}$$

where $E(\cdot)$ denotes the statistical expectation over time. Assuming ergodicity and uncorrelated noise at the elements, (39) becomes

$$\text{SNR}_{\text{in}} = \frac{\mathbf{v}_{\mathbf{ideal}}{}^H C^H C\mathbf{v}_{\mathbf{ideal}}}{N\sigma_o^2}, \tag{40}$$

where σ_o^2 is the noise power. As illustrated in Figure 4, the signal at the output of the processor is given by

$$y = \mathbf{w}^H\mathbf{v} = \mathbf{w}^H C\mathbf{v}_{\mathbf{ideal}} + \mathbf{w}^H\mathbf{n}, \tag{41}$$

where the column vector $\mathbf{w}$ contains the weights applied to each of the elements. Using (41), the SNR_{out} in (37) is obtained by

$$\begin{aligned}\text{SNR}_{\text{out}} &= E\left(\frac{|\mathbf{w}^H C\mathbf{v}_{\mathbf{ideal}}|^2}{|\mathbf{w}^H\mathbf{n}|^2}\right)\\ &= E\left(\frac{\mathbf{v}_{\mathbf{ideal}}{}^H C^H\mathbf{w}\mathbf{w}^H C\mathbf{v}_{\mathbf{ideal}}}{\mathbf{w}^H\mathbf{n}\mathbf{n}^H\mathbf{w}}\right).\end{aligned} \tag{42}$$

Since the noise is uncorrelated, $E(\mathbf{n}\mathbf{n}^H) = \sigma_o^2 I$, and (42) reduces to

$$\text{SNR}_{\text{out}} = \frac{\mathbf{v}_{\mathbf{ideal}}{}^H C^H\mathbf{w}\mathbf{w}^H C\mathbf{v}_{\mathbf{ideal}}}{\sigma_o^2\mathbf{w}^H\mathbf{w}}. \tag{43}$$

Substituting (40) and (43) into (37) yields

$$A = N\frac{\mathbf{v}_{\mathbf{ideal}}{}^H C^H\mathbf{w}\mathbf{w}^H C\mathbf{v}_{\mathbf{ideal}}}{\mathbf{w}^H\mathbf{w}\mathbf{v}_{\mathbf{ideal}}{}^H C^H C\mathbf{v}_{\mathbf{ideal}}}. \tag{44}$$

Recently, [18, 19] demonstrated that adaptive beamforming based on the minimum-mean-square-error (MMSE) algorithm only gains a slight improvement in convergence rate as a result of MCC. It is found that MCC does not yield a lower mean square error (MSE) between the array output and the reference signal in the steady state. Similarly, the array gain in (44), provided by adaptive array processing, converges to the same value as that in the absence of MCC. However, in certain applications, the signal statistics change too rapidly for adaptive array processing to be effective. For DOA estimation, adaptive processing is also generally not an option. It is, therefore, insightful to evaluate MCC methods in the deterministic case where the signal statistics are known. The optimum weights in the deterministic case are simply given by

$$\mathbf{w} = \widetilde{C}\mathbf{v}_{\mathbf{ideal}}. \tag{45}$$

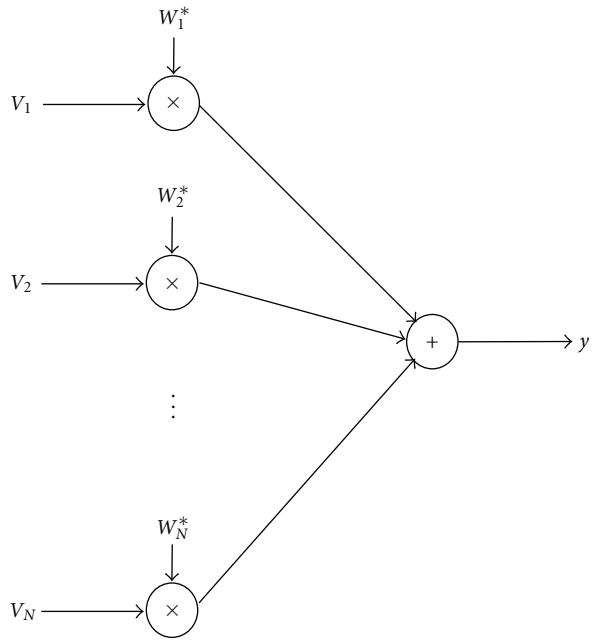

Figure 4: General smart antenna block diagram. The terminal voltages of the array elements are individually multiplied by the conjugated weights. The summation of the weighted voltages yields the smart antenna output y.

In the absence of mutual coupling, $\widetilde{C} = I$, and the weights in (45) can be verified to be equal to those generally employed in conventional uniformly weighted phased arrays. If the coupling matrix is perfectly known, $\widetilde{C} = C$, and the use of $\mathbf{w}$ in (45) ensures that the required signals are added coherently based on the relative phases of the signals at each element contained in $C\mathbf{v_{ideal}}$. By multiplying the conjugate of each weight with $C\mathbf{v_{ideal}}$ in (41), the phases of the required signals are verified to vanish, and the output SNR is maximized. Substituting (45) into (44), the array gain becomes

$$A = N\frac{\mathbf{v_{ideal}}^H C^H \widetilde{C}\mathbf{v_{ideal}}\mathbf{v_{ideal}}^H \widetilde{C}^H C\mathbf{v_{ideal}}}{\mathbf{v_{ideal}}^H \widetilde{C}^H \widetilde{C}\mathbf{v_{ideal}}\mathbf{v_{ideal}}^H C^H C\mathbf{v_{ideal}}}. \tag{46}$$

It is verified that when $\widetilde{C} = C$, (46) reduces to $A = N$. In other words, in the perfect knowledge of the coupling matrix, the optimum array gain is achieved, and it is equal to the number of elements. When mutual coupling is ignored and no MCC is implemented, the coupling matrix is assumed to be $\widetilde{C} = I$. The weights are then given by $\mathbf{w} = \mathbf{v_{ideal}}$, and the array gain is

$$A = N\frac{\mathbf{v_{ideal}}^H C^H \mathbf{v_{ideal}}\mathbf{v_{ideal}}^H C\mathbf{v_{ideal}}}{\mathbf{v_{ideal}}^H \mathbf{v_{ideal}}\mathbf{v_{ideal}}^H C^H C\mathbf{v_{ideal}}}. \tag{47}$$

In the next three subsections, (46) is used to evaluate the performance of the open-circuit voltage, calibration and receiving mutual impedance methods for the nineelement planar array. As discussed in Section 2.3, since the coupling matrix calculated using the full-wave method approaches the actual coupling matrix when the numerical model is accurate, the array gain obtained following MCC based on this method approaches N in general, and 9 in the specific case of the nineelement array. Therefore, the full-wave method is used here as a reference to evaluate the other three methods. The array gain obtained using each method is also compared against that obtained in the absence of MCC as given by (47). For all the MCC methods, the estimated coupling matrix $\widetilde{C}$ is calculated based on currents computed using NEC at 51 different frequencies within the operating frequency range of the dipoles. The array gain is calculated using (46) for a signal known to be arriving from $\phi = 0^\circ$ and $\theta = 90^\circ$, that is, from the positive x-axis.

3.1. Open-Circuit Voltage Method Performance. As described in Section 2.1, the coupling matrix can be estimated by successively exciting one of the array elements with a voltage source at its terminals while all the other elements are short circuited. For the nine-dipole array, this technically requires nine different calculations. Since the nine dipoles are identical and are terminated into equal load impedances, symmetry can be used advantageously to reduce the number of calculations. Based on symmetry, the currents resulting from only three different configurations need to be calculated. As shown in Figure 5(a), a voltage source is first applied at the terminals of element 8, and the currents in the segments corresponding to the shorted terminals of the other elements are calculated. These are used to fill the column numbered 8 of the mutual admittance matrix according to (7). Thanks to symmetry, the entries of column 8 can be reused to fill columns 2, 4, and 6. Similarly, by exciting element 7 as illustrated in Figure 5(b), columns 1, 3, 7, and 9 of the mutual admittance matrix are filled. Finally, by exciting element 5 as shown in Figure 5(c), column 5 of the mutual admittance matrix is filled. The mutual admittance matrix is then inverted according to (8) to obtain the mutual impedance matrix, which is then substituted into (5) to calculate $\widetilde{C}$. Since the nine elements are to be terminated into 300 Ω, Z_L in (5) is given by $300I$.

The coupling matrix estimate calculated at the 51 different frequencies is substituted into (46) to calculate the resulting array gain. The result is shown in Figure 6. The array gain using the open-circuit voltage method is seen to provide a significant improvement over the uncompensated case for frequencies below $d \approx 0.2\lambda$. These include the first resonant frequency at $d \approx 0.1875\lambda$. This result is consistent with most previously published work where the analysis was done at frequencies where the elements were generally half-wave dipoles and, thereby, operating at first resonance. Although the electrical spacing of the elements is smaller at the first resonant frequency for the array being studied in this paper, there is, nevertheless, some performance improvement. However, the performance degrades significantly as frequency increases, reaching a minimum array gain of approximately 4.5 at $d \approx 0.3\lambda$. Between $d \approx 0.2\lambda$ and $d \approx 0.43$, a detrimental effect of implementing MCC using the open-circuit voltage is observed since ignoring mutual coupling would yield better performance. The method is seen to yield results that are highly dependent on frequency.

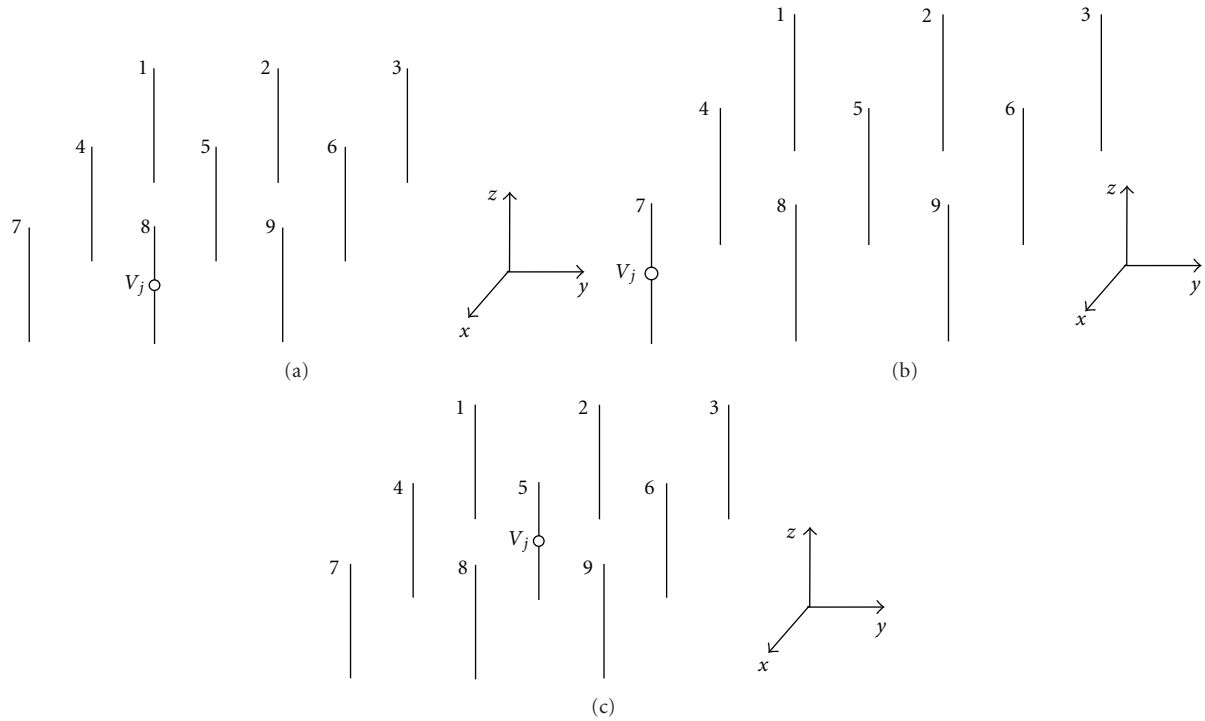

Figure 5: Required calculations for the open-circuit voltage method based on symmetry considerations. In (a), induced terminal currents by the excitation of element 8 using a voltage source are used for those by the excitation of elements 2, 4, and 6. In (b), induced terminal currents by the excitation of element 7 are used for those by the excitation of elements 1, 3, and 9. Finally in (c), induced terminal currents by the excitation of element 5 are only used for this element since no other element has the same surrounding electromagnetic environment.

The only frequencies where the array gain approaches that for the full-wave method are the lowest frequencies. As discussed in Section 2.1, this is expected since for small electrical dimensions of the elements, the excitation can be approximated as being only at the terminals. It was shown in Section 2.3 that when this approximation is valid, then the open-circuit voltage method yields accurate results.

3.2. Calibration Method Performance. An important consideration in the implementation of the calibration method is the number of calibration points selected. As mentioned in Section 2.2, a number of calibration points equal to at least the number of elements is required to obtain a unique solution to (13). However, depending on the complexity of the array, this number may not be sufficient to obtain an accurate coupling matrix estimate. For the nine-dipole array, nine calibration points were found to be insufficient when they are equispaced over 360° beginning at 0°. However, the implementation of [13, 14], discussed in Section 2.4, was verified to give satisfactory performance with as little as nine calibration points. The array gain obtained using the implementation of Section 2.2 with 16, 18, and 360 calibration points is shown in Figure 7. In each case, the terminal voltages are calculated under plane wave external excitation over 360° beginning at 0°. The azimuth intervals are given by 22.5°, 20°, and 1°, respectively.

It is observed that the resulting performance using only 16 calibration points shows important variations with respect to frequency. The number of calibration points is visibly too small. It is interesting to see that adding only two calibration points yields a much better performance where the array gain is seen to reach the optimal value of 9 at $d \approx 0.12\lambda$ and remains constant as frequency increases. Increasing the number of points even more has the effect of reducing the frequency at which the optimal array gain is reached. For 360 calibration points, the array gain is, therefore, very close to 9 at the lowest frequency of interest. When the number of calibration points is too small, $V_{\text{ideal}} V_{\text{ideal}}{}^H$ in (14) has a high condition number. Consequently, $\widetilde{C}$ is inaccurate and yields suboptimal performance. This problem is exacerbated at lower frequencies since the phase shifts between the signals in V_{ideal} are smaller. The only way to ensure that $\widetilde{C}$ is accurate is by increasing the number of calibration points. As indicated by the above example, if some performance tradeoffs are acceptable, especially at low frequencies, it is possible to limit the number of points to a reasonable value in order to reduce the amount of computations or measurements.

3.3. Receiving Mutual Impedance Method Performance. Similar to the open-circuit voltage method in Section 3.1, the receiving mutual impedance method necessitates multiple calculations for the determination of the mutual impedances given by (30). Although several variants are found in the literature for determining the receiving mutual impedances, including one where all of the elements are simultaneously excited by a plane wave instead of exciting each element

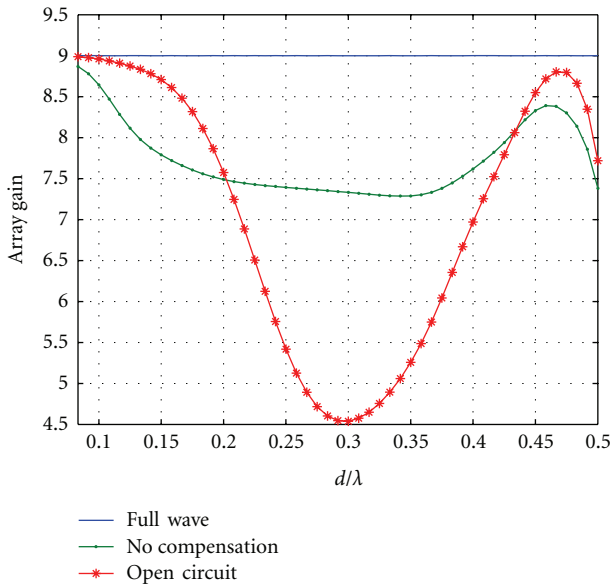

Figure 6: Array gain using the open-circuit voltage method as a function of the electrical separation (d/λ) between the elements of the nine-dipole planar array for a signal arriving from $\phi = 0°$. Maximum gain is achieved as $d/\lambda \to 0$. The implementation of the open-circuit voltage method yields a degradation in performance between $d \approx 0.2\lambda$ and $d \approx 0.43$, where the gain reaches lower magnitudes than those of the uncompensated case.

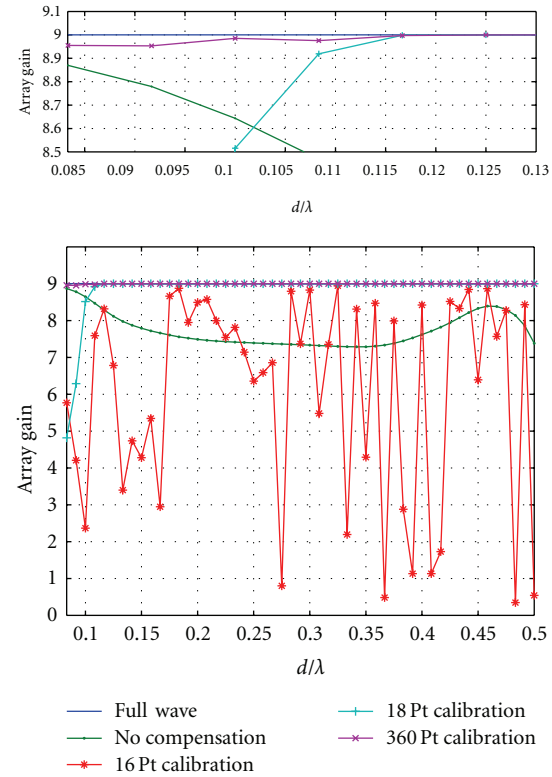

Figure 7: Array gain using the calibration method as a function of the electrical separation (d/λ) between the elements of the nine-dipole planar array for a signal arriving from $\phi = 0°$. The performance of the calibration method is dependent on the number of calibration points. Instability in the estimation of the coupling matrix yields erratic performance for 16 calibration points. Maximum gain is reached at lower frequencies as the number of calibration points increases.

pair separately, the element pairs are treated separately here for better accuracy. This implementation of the method technically first requires N calculations where each element is excited separately in the receiving mode. Then $N(N-1)$ more calculations are required to calculate V_{ij} in (30) for the $N-1$ elements excited by the N different I_j. Therefore, a total of N^2 different calculations are required. By taking advantage of symmetry, this number can be reduced to six for the nine-dipole array to take into consideration all the different configurations of element pairs. The six different configurations used in the calculations are illustrated in Figure 8. Since the nine dipoles are identical and are terminated into equal load impedances, only one element needs to be excited separately. In Figure 8(a), element 9 is arbitrarily selected for the separate excitation. Then, in Figures 8(b)–8(f), Z_{95}, Z_{96}, Z_{92}, Z_{93}, and Z_{91} are calculated, respectively, according to (30). Based on symmetry, these mutual impedances are then reused to completely fill the coupling matrix estimate in (34) where the load impedances, Z_{L_i}, are replaced with 300 Ω. To verify whether the assumption stated in Section 2.4 that the current distributions are independent of the excitation DOA, $\widetilde{C}$ is calculated for excitation DOAs of 0°, 45°, 90°, and 135°. The array gain obtained using the four different excitation DOAs is shown in Figure 9.

The performance of the receiving mutual impedance method is observed to be impressively good for frequencies below $d \approx 0.3\lambda$ where the gain approaches the optimal value for any excitation DOA. At higher frequencies, there is a degradation in performance although it remains superior to that when no MCC is implemented. Also, the performance becomes dependent on the excitation DOA used in the calculation of $\widetilde{C}$. An excitation DOA of $\phi = 90°$ is seen to provide the best results among the four DOAs up to $d \approx 0.43\lambda$, and an excitation DOA of $\phi = 135°$ provides the best results above this frequency. The degradation in performance and the dependence on the excitation DOA are explained by the incorrect assumption that the current distributions are unaffected by the presence of the other elements, as discussed in Section 2.4. Due to the alteration of the current distributions when the elements are in the presence of one another, the symmetry used in filling $\widetilde{C}$ is also questionable.

4. Performance Comparison of Mutual Coupling Compensation Methods for Arbitrary Elevation Angle

Finally, the performance of the MCC methods can be compared for signals arriving from $\theta \neq 90°$. As mentioned in Section 2.4, an important advantage of the receiving mutual impedance method over the full-wave method is that no assumption needs to be made with respect to the elevation angle of incoming signals. To verify the relevance

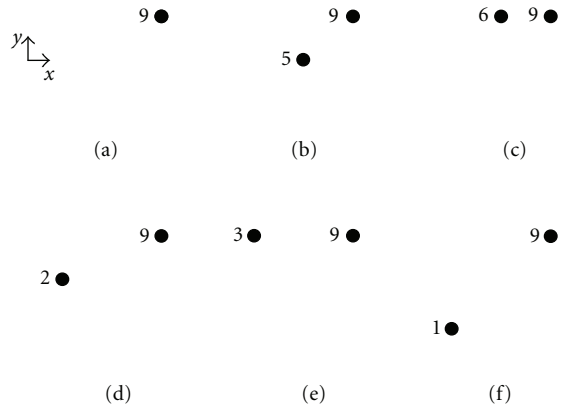

Figure 8: Required calculations for the receiving mutual impedance method based on symmetry considerations. In (a), the induced terminal current by the excitation of element 9 in the absence of the other elements using an external incident plane wave is calculated. In (b)–(f), the induced terminal voltages of elements 5, 6, 2, 3, and 1 are separately calculated in the presence of element 9. The six calculations are sufficient to fill the coupling matrix estimate completely.

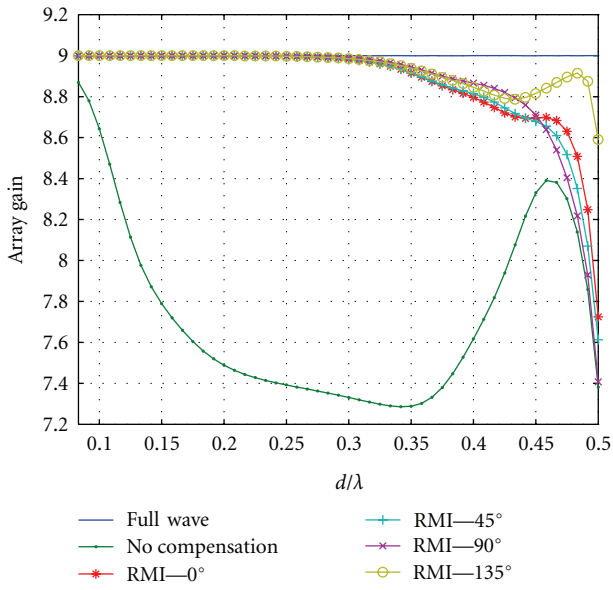

Figure 9: Array gain using the receiving mutual impedance (RMI) method as a function of the electrical separation (d/λ) between the elements of the nine-dipole planar array for a signal arriving from $\phi = 0°$. Maximum gain is achieved for $d/\lambda < 0.3$. The performance degrades as frequency increases and becomes dependent on the excitation DOA used in the computation of the coupling matrix estimate. Nevertheless, it is superior to that of the uncompensated case for all the plotted frequencies.

of this, the array gain is calculated for the nine-dipole array with an incoming signal arriving from $\phi = 0°$ and $\theta = 45°$. Although the coupling matrix can be estimated accurately using the full-wave method in the deterministic case, the coupling matrix calculated for $\theta = 90°$ is used to evaluate the impact of relying on the same coupling

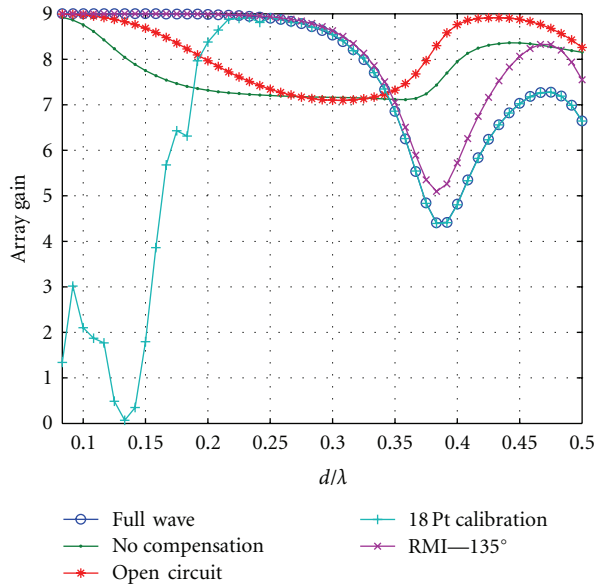

Figure 10: Array gain as a function of the electrical separation (d/λ) between the elements of the nine-dipole planar array for a signal arriving from $\phi = 0°$ and $\theta = 45°$ using the various mutual coupling compensation methods. Maximum gain is achieved for $d/\lambda < 0.25$ using the full-wave and receiving mutual impedance methods (RMI). The performance of the two methods degrades as frequency increases. The RMI method is slightly superior to the full-wave method for the plotted frequencies. For $d/\lambda > 0.35$, the open-circuit method is superior to all the other methods.

matrix regardless of the elevation angle. The coupling matrix estimated using 18 points is selected for this example since it provided satisfactory results in Section 3.2. For the receiving mutual impedance method, the excitation DOA of 135° is selected based on its best overall wideband performance in Section 3.3. The results are shown in Figure 10.

For this value of elevation angle, the receiving mutual impedance method is observed to provide nearly optimal gain up to $d \approx 0.25\lambda$. Compared to the performance obtained for $\theta = 90°$, there is a reduction in the bandwidth over which the method yields optimal results. Beyond $d \approx 0.35\lambda$, the implementation of the method is seen to be detrimental since it yields a significantly lower gain than without MCC, except for a narrow range of frequencies around $d \approx 0.475\lambda$. However, it is verified that the receiving mutual impedance method is superior to the full-wave method over all the plotted frequencies. Unfortunately, the improvement in performance is very small, reaching approximately 2.5% over the range of frequencies where the two methods are superior to all the other methods. Beyond $d \approx 0.35\lambda$, it is simply better to use the open-circuit voltage method since it provides better performance.

The performance degradation of MCC methods observed in this section is explained as follows. The vertical phase shifts of incident signals along the array elements become more important as the frequency increases, causing square coupling matrices to be less accurate in quantifying mutual coupling for all elevation angles. For array elements

having large horizontal dimensions, such as some printed circuit type antennas, horizontal phase shifts of the incident signals are an additional complication. Mutual coupling in such antennas, as well as vertical wire antennas illuminated by signals of arbitrary elevation, may be better described by nonsquare coupling matrices, as discussed in [11].

5. Conclusions

Various mutual coupling compensation methods were compared over a wide range of frequencies. Through the accurate quantification of their wideband performance, their limitations were outlined. It was shown that only the full-wave method yields accurate results at all frequencies, provided that the numerical model is accurate. The open-circuit voltage method is only accurate when the elements are electrically small and was shown to yield a performance approaching that of the full-wave method when the array elements can be approximated by a single segment. Although the receiving mutual impedance method is accurate over a larger range of frequencies, its performance degrades significantly when the array elements become electrically larger. For example, it was shown that the method is not accurate for dipoles operating at the second resonant frequency. Due to the resulting instability in the computation of the coupling matrix estimate, the calibration method is less accurate and requires a larger number of calibration points when the distance between the array elements becomes electrically small. The only limitation of the full-wave method with respect to the other three methods is that the coupling matrix can generally only be evaluated theoretically. The other methods can evaluate the matrix experimentally, but the required number of measurements was shown to vary, with the open-circuit voltage method requiring the least. It was demonstrated that the receiving mutual impedance method only provides a marginal advantage over the full-wave method in the sense that it does not require *a priori* information on the elevation angle of incoming signals. The results presented here can be useful for both wideband and narrowband receiving antenna arrays.

References

[1] H. T. Hui, "Decoupling methods for the mutual coupling effect in antenna arrays: a review," *Recent Patents on Engineering*, vol. 1, no. 2, pp. 187–193, 2007.

[2] I. J. Gupta and A. A. Ksienski, "Effect of mutual coupling on the performance of adaptive arrays," *IEEE Transactions on Antennas and Propagation*, vol. AP-31, no. 5, pp. 785–791, 1983.

[3] J. Pierre and M. Kaveh, "Experimental performance of calibration and direction-finding algorithms," in *Proceedings of the IEEE International Conference on Acoustics, Speech and Signal Processing (ICASSP '91)*, vol. 2, pp. 1365–1368, Toronto, Canada, 1991.

[4] R. S. Adve and T. K. Sarkar, "Compensation for the effects of mutual coupling on direct data domain adaptive algorithms," *IEEE Transactions on Antennas and Propagation*, vol. 48, no. 1, pp. 86–94, 2000.

[5] H. T. Hui, "Compensating for the mutual coupling effect in direction finding based on a new calculation method for mutual impedance," *IEEE Antennas and Wireless Propagation Letters*, vol. 2, pp. 26–29, 2003.

[6] S. Henault and Y. M. M. Antar, "Comparison of various mutual coupling compensation methods in receiving antenna arrays," in *Proceedings of the IEEE International Symposium on Antennas and Propagation and USNC/URSI National Radio Science Meeting*, Charleston, SC, USA, 2009.

[7] P. S. Carter, "Circuit relations in radiating systems and applications to antenna problems," *Proceedings of the IRE*, vol. 20, 1932.

[8] J. D. Kraus, *Antennas*, McGraw-Hill, New York, NY, USA, 2nd edition, 1988.

[9] R. F. Harrington, *Field Computation by Moment Methods*, Wiley, New York, NY, USA, 1968.

[10] H. S. Lui, H. T. Hui, and M. S. Leong, "A note on the mutual-coupling problems in transmitting and receiving antenna arrays," *IEEE Antennas and Propagation Magazine*, vol. 51, no. 5, Article ID 5432083, pp. 171–176, 2009.

[11] S. Henault, Y. M. M. Antar, S. Rajan, R. Inkol, and S. Wang, "The multiple antenna induced emf method for the precise calculation of the coupling matrix in a receiving antenna array," *Progress in Electromagnetics Research M*, vol. 8, pp. 103–118, 2009.

[12] H. T. Hui, "A practical approach to compensate for the mutual coupling effect in an adaptive dipole array," *IEEE Transactions on Antennas and Propagation*, vol. 52, no. 5, pp. 1262–1269, 2004.

[13] H. S. Lui and H. T. Hui, "Improved mutual coupling compensation in compact antenna arrays," *IET Microwaves, Antennas and Propagation*, vol. 4, no. 10, pp. 1506–1516, 2010.

[14] H. S. Lui and H. T. Hui, "Mutual coupling compensation for direction-of-arrival estimations using the receiving-mutual-impedance method," *International Journal of Antennas and Propagation*, vol. 2010, Article ID 373061, 7 pages, 2010.

[15] Institute of Electrical and Electronics Engineers, IEEE 100, *The Authoritative Dictionary of IEEE Standards Terms*, IEEE Press, New York, NY, USA, 7th edition, 2000.

[16] *NEC-2 Manual*, Lawrence Livermore National Laboratory, 1996.

[17] H. L. van Trees, *Optimum Array Processing (Detection, Estimation, and Modulation Theory, Part IV)*, New York, New York, NY, USA, 2002.

[18] Q. Yuan, Q. Chen, and K. Sawaya, "Performance of adaptive array antenna with arbitrary geometry in the presence of mutual coupling," *IEEE Transactions on Antennas and Propagation*, vol. 54, no. 7, pp. 1991–1996, 2006.

[19] Z. Huang and C. A. Balanis, "The MMSE algorithm and mutual coupling for adaptive arrays," *IEEE Transactions on Antennas and Propagation*, vol. 56, no. 5, pp. 1292–1296, 2008.